JOURNAL OF CATALYSIS **161,** 164–177 (1996)
ARTICLE NO. 0173

Catalytic Hydrodechlorination of CCl_4 over Silica-Supported $PdCl_2$-Containing Molten Salt Catalysts: The Promotional Effects of $CoCl_2$ and $CuCl_2$

Xi Wu, Yakov A. Letuchy, and Darrell P. Eyman[1]

Department of Chemistry, University of Iowa, Iowa City, Iowa 52242

Received April 28, 1995; revised January 8, 1996; accepted February 9, 1996

The hydrodechlorination of CCl_4 with H_2 was tested over several silica-supported $PdCl_2$-containing molten salt catalysts. The base catalyst was $PdCl_2$–$(C_4H_9)_4NCl/SiO_2$; $CoCl_2$, $CuCl_2$, or both were doped into the catalyst as promoters to modify its activity, product selectivity, and catalyst longevity. The catalysts converted CCl_4 into C_1–C_5 paraffins and C_2–C_4 olefins, CH_2Cl_2, $CHCl_3$, CCl_2CCl_2, and $CHClCCl_2$. Doping $CoCl_2$ into the $PdCl_2$–$(C_4H_9)_4NCl/SiO_2$ catalyst enhances its initial CCl_4 conversion from 85 to 99.3%, shifts reaction products toward more hydrocarbons, and also prolongs the life of the catalyst. Addition of $CuCl_2$ to the $PdCl_2$–$(C_4H_9)_4NCl/SiO_2$ catalyst also improves the initial CCl_4 conversion to 94.5% and has an even stronger stabilizing effect on the catalytic activity, while shifting reaction products toward C_1-chlorocarbons. When both $CoCl_2$ and $CuCl_2$ are added to the base catalyst, the promoted catalyst exhibits the highest CCl_4 initial conversion of 99.5% and the greatest longevity among all four catalysts. The corresponding specific activities for the above catalysts were of 0.636×10^{-3}, 1.154×10^{-3}, 1.139×10^{-3}, and 1.184×10^{-3} mol CCl_4/g cat min at 130°C, respectively. The promotional and product distribution effects were attributed to the presence of $CoCl_2$, $CuCl_2$, or both as additional Lewis acidic sites for activation of CCl_4 molecules and to the interaction of these additives with the Pd-containing active centers in supported molten salt media.

INTRODUCTION

Containment and destruction of environmentally hazardous halocarbons are of great importance in protecting the atmospheric ozone layer and reducing harmful air pollution. One promising approach is to use hydrogen to convert them catalytically into hydrocarbons. Hydrodechlorination of CCl_4 with H_2 has been reported in the literature on conventional heterogeneous supported Group VIII metal catalysts. Among all volatile chlorocarbons carbon tetrachloride is the most difficult one to be catalytically hydrodechlorinated because of its fouling on these catalysts. These catalysts may be active initially but have relatively short useful life.

Weiss and co-workers (1) studied the kinetics and selectivity of this reaction on Pt/Al_2O_3 using a differential mode for catalyst testing, i.e., the CCl_4 conversion was maintained at low levels (<8%). In a temperature range of 12–123°C and a pressure range of 60–790 Torr, they measured an activation energy of 19.25 kcal/mol and found $CHCl_3$ and CH_4 to be the main products from the reaction, with only trace quantities of CH_2Cl_2 and CH_3Cl. They proposed that the formation of $\cdot CCl_3$ radical in the initiation step followed by addition of a hydrogen atom to $\cdot CCl_3$ accounts for $CHCl_3$ while concerted, rather than sequential, hydrogen addition to the adsorbed $\cdot CCl_3$ accounts for CH_4. Weiss and co-workers (2) also studied the hydrodechlorination and oligomerization of CCl_4 on Ni/Y zeolites using a pulsed microreactor. At a reaction temperature of 370°C the coversion was initially high but the catalysts were deactivated very rapidly. The observed high selectivity toward CCl_3CH_2Cl (up to 40%) was attributed to an oligomerization–termination step between $\cdot CCl_3$ and $\cdot CH_2Cl$ following the sequential free-radical propagation steps from CCl_4. The overall reaction rate, in turnover frequency, was estimated to be less than 0.01 mol CCl_4 converted per mole surface Pt per second.

The technique of carbon skeleton gas chromatography (3) was also used to study the hydrodechlorination of a diluted mixture of CH_2Cl_2, $CHCl_3$, CCl_4 (1000–2000 ppm in heptane). In this case, salts of all Group VIII transition metals except Os were impregnated on Gas-Chrom Q GC-column material to form the supported catalysts. The test results showed 97–99% conversion of these chlorocarbons and up to 97.7% product selectivity toward CH_4 for the most active Pd catalyst at 170°C. The turnover rate was estimated to be less than 0.06 mol CCl_4 converted per mole surface Pd per second at this temperature.

In a study by Drago and co-workers (4), novel catalysts with strong acid sites were prepared by sequential treatment of silica gel with a noble metal salt such as $PdCl_2$, K_2PdCl_4, $RhCl_3$, or $RuCl_3$ along with strong Lewis acids such as $AlCl_3$ and/or $ZnCl_2$. These new solid acid catalysts exhibit high catalytic activity for hydrodechlorination

[1] To whom correspondence should be addressed.

0021-9517/96 $18.00

of CCl_4 and dehydrochlorination/hydrodechlorination of CH_2ClCH_2Cl. One catalyst, prepared by treatment of silica gel support with $PdCl_2$ and then with $AlCl_3$, exhibited both high activity and selectivity for hydrodechlorination of CCl_4 toward $CHCl_3$ at 90°C and atmospheric pressure. Another catalyst prepared by a reverse procedure, i.e., treating silica first with $AlCl_3$ and then with $PdCl_2$, converted CCl_4 at the same reaction condition to hydrocarbons, with up to 10.1% of $CHCl_3$ appeared after 9 h on stream. However, these catalysts were unstable and deactivated after about 18 h at 90°C and much faster at 110°C.

Supported molten salt catalysis (SMSC) is a special adaptation of supported liquid phase catalysis (SLPC) (5–12). SLPC incorporates a liquid containing dissolved or dispersed catalyst, which coats the walls of the pores in the support. Gaseous or vapor phase reactants diffuse through the residual pore space, dissolve in the liquid phase, and react at catalyst sites within the thin liquid film. The products then diffuse back out of the thin film into the void pore space and out of the support. The SLPC technique combines the attractive features of homogeneous catalysis, such as high specificity and molecular dispersion of the catalyst, with those of heterogeneous catalysis, such as large interfacial area, less corrosion, ease of separation of products and catalysts, and use of conventional reactors. Diffusional problems normally found for reactions of gaseous reactants in bulk liquids are almost nonexistent in the SLPC method because of the thickness of the thin film (50 Å or less).

However, the SLPC method requires that the catalyst liquid phase and all of its dispersed components must be essentially nonvolatile; the use of molten salt eutectics as the liquid phase reaction medium overcomes the solution volatility problem. A large variety of molten salt eutectics is available with melting points ranging from below 50°C to above 1000°C (13, 14). These molten salt eutectics have been used as the liquid phase for dispersion of transition metals, metal oxides, and metal complex catalysts. The SMSC technique is potentially applicable to any gaseous or vapor phase reaction system over a temperature range which is limited only by the melting point of the molten salt eutectic or the thermal stability of the dispersed catalyst. Inorganic molten salts, especially chloride salts, are commonly used to form molten media.

The use of organic molten salts such as tetraethylammonium or tetrabutylammonium cations with trichlorostannate or trichlorogermanate counterions as media for hydrogenation catalysts was first reported by Parshall (15). These catalysts included both elemental Pt or 5-coordinate complexes such as $[Pt(SnCl_3)_5]^{3-}$ and $[HPt(SnCl_3)_4]^{3-}$. A phosphonium salt, $(C_6H_5)_3CH_3PSnBr_3$, was used as well. Among other hydrogenation and carbonylation reactions, these catalysts were used for hydrodechlorination of vinyl chloride to ethane at a pressure of about 2 atm and 105–120°C. It was further shown that catalysts containing water-soluble triphenylalkylphosphonium chlorides or bromides incorporated into an activated carbon support together with salts of copper and palladium or rhodium acted as catalysts for the selective hydrodechlorination of CCl_4 to $CHCl_3$ (16). The state of the salts in a catalyst consisting of $CuCl_2$, Na_3RhCl_6, and $(C_6H_5)_3CH_3PCl$ (10 wt% Cu, 0.044 wt% Rh, and 6.5 wt% $(C_6H_5)_3CH_3PCl$) supported on carbon and operated at 200°C and 4 bar was not disclosed, but we assume that part of the catalyst exists as a molten salt. However, at the low $(C_6H_5)_3CH_3PCl$ to Cu molar ratio described, we also suspect that at least part of the copper was present in the solid state as Cu(II) and Cu(I) salts, or elemental Cu.

Our research work focuses on the use of silica-supported $PdCl_2$-containing molten salt catalysts to study the hydrodechlorination of CCl_4. Tetrabutylammonium chloride was chosen as the main molten medium because of its low melting point (42°C) and its relatively good stability. A $PdCl_2$–$(C_4H_9)_4NCl/SiO_2$ molten salt catalyst will form the basis for comparison with other similar catalysts promoted by addition of either $CoCl_2$ or $CuCl_2$ or both. In this study we report our findings on these catalysts including their activity, product distribution, and stability.

EXPERIMENTAL

Materials

The chloride salts used as catalyst precursor compounds included palladium (II) chloride ($PdCl_2$), cobalt (II) chloride hydrate ($CoCl_2 \cdot 6H_2O$), copper (II) chloride hydrate ($CuCl_2 \cdot xH_2O$), and tetrabutylammonium chloride hydrate $(C_4H_9)_4$ NCl·H_2O. Palladium (II) chloride was purchased from Johnson Matthey, cobalt (II) chloride was from EM Science, and copper (II) chloride and tetrabutylammonium chloride were from Aldrich. The copper (II) chloride was dried at 110°C to remove H_2O before weighing. The silica support (CS-1022) with high purity and large pores was donated by the PQ Corporation. It has a N_2 pore volume of 1.35 cm^3/g, an average pore radius of 125 Å, and a surface area of 200 m^2/g. The SiO_2 particles were crushed and sieved to 40–60 mesh size before use in catalyst preparation. The GR-grade carbon tetrachloride was purchased from EM Science. Both H_2 gas (>99.8%) and He gas (>99.99%) were obtained from Air Products; each gas was further purified by passing it through a gas drier and an oxygen trap (Alltech).

Catalyst Preparation

All catalysts were prepared by the method of incipient wetness impregnation. The chloride salts, weighed to appropriate amounts, were dissolved in a flask with an excess amount of methanol that had a few drops of concentrated HCl added to it. The dissolution of $PdCl_2$ in methanol was

slow compared to other chloride salts and required constant stirring of the solution for up to 10 h. Fresh methanol was added occasionally to maintain the same solution volume during this process. After all chloride salts were completely dissolved, excess methanol was allowed to evaporate to reduce the volume of the solution. No crystallization or precipitation was observed during evaporation, and the solution remained clear (orange-yellow for $PdCl_2$ and $CuCl_2$ solution; green for $CoCl_2$-containing solution). The silica support was dried at 110°C for 2 h before use. The volume of the solution necessary for impregnation was estimated based on the total pore volume of the silica support and also from a blank test with only methanol. This was about 3 ml solution per gram dried SiO_2. The SiO_2 particles were added to the solution for impregnation; the solution containing the chloride salts was drawn into the support pores by simple capillary action. The material was left standing in open air (under a fume hood) to dry overnight, and then it was further dried at 120°C for 1 h.

Microreactor System

The testing of catalysts for hydrodechlorination of CCl_4 was carried out in a microreactor system shown in the schematic diagram in Fig. 1. It consisted of four major components: (i) the inlet gas and liquid feed lines with flow control devices, (ii) a reactor tube with an IR heating furnace, (iii) a reactor exit pressure/flow control assembly with a gas sampling valve, (iv) a computer-controlled GC. The flow rates for the two gases used in this study, H_2 and He, were each controlled by mass flow controllers (Brooks Instrument, Model 5850E) with a flow range of 0–250 sccm. CCl_4 as a liquid at ambient temperature was delivered at a precise flow rate by a liquid syringe pump (ISCO, Model LC-5000). The liquid was vaporized in the transfer line heated by heating tapes (at about 120°C) before mixing with the H_2 gas. The transfer line from the point of mixing to the reactor inlet was also heated and the temperature was maintained at about 120°C to avoid condensation of CCl_4. The 12″ reactor tube was 3/8″ o.d. and had extension tubes connected on both ends via VCR-type connection with ring gaskets for ease of catalyst loading and removal. A preheater was coiled around the exterior of the reactor tube. The reactor tube was placed along the axial center within the focal zone of a quad-elliptical infrared heating chamber (Research, Inc., Model E4-25). The outer surfaces of the reactor tube and the preheater tube were preoxidized in air (blackened) to reduce IR reflectivity and enhance IR absorptivity. The temperature of the catalyst bed, which was located in the center section of the reactor tube, was measured directly by an inserted thermocouple and was monitored and controlled by a temperature controller (Omega, Model CN-2011). The reactor outlet flow was regulated by two metering valves, and the transfer line was heated to about 135°C to avoid condensation of any C_2-chlorocarbons formed as reaction products. A pneumatically actuated six-port gas sampling valve provided on-line gas sampling to a gas chromatograph. The gas chromatograph (HP 5890 Series II, Hewlett–Packard) was equipped with a 5′ × 1/8″ o.d. nickel tubing column packed with 100–120 mesh HayeSep R polymer beads (Alltech), and the products were detected by TCD. The GC data were collected through an advanced computer interface (Dionex) connected to a 486DX/33 PC.

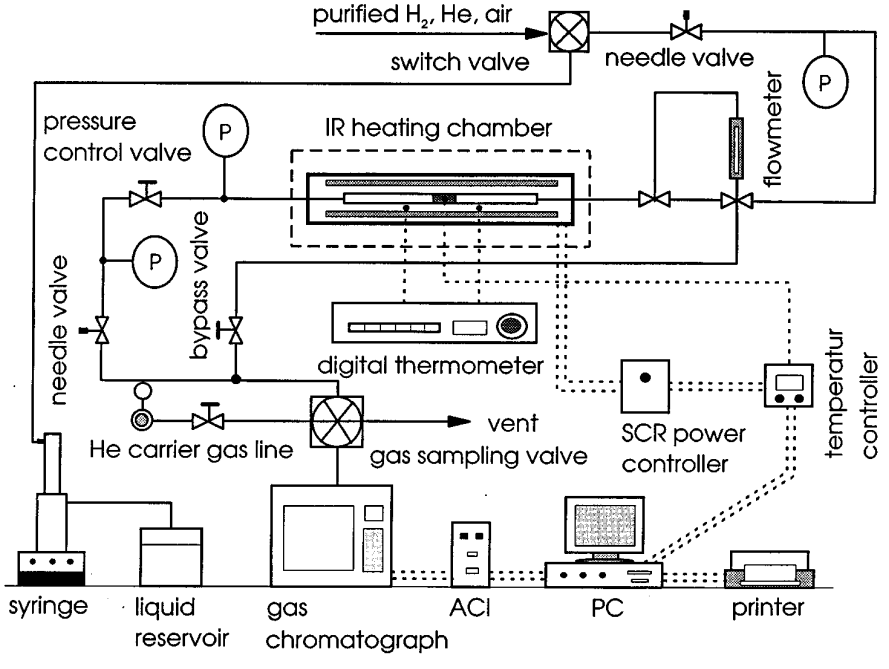

FIG. 1. A schematic diagram of a microreactor system.

All GC data processing was performed using Dionex GC software.

Catalyst Testing

The reactor tube was partially filled with coarse SiC particles (about 20 mesh) on the exit end held between quartz wool plugs to help position the catalyst bed near the center section of the tube. For catalyst tests in the integral mode, the catalyst bed consisted of about 0.6 g of catalyst particles diluted in about 4.5 g of 40–60 mesh SiC particles (about 2.5 cm^3 in volume). This mixture was packed into the reactor and held in place between quartz wool plugs. The catalyst was first pretreated with 30 sccm of He gas at 120°C for about 1 h to purge the system, remove air and moisture from the catalyst, and also to homogenize the molten salts inside the silica pores. The temperature of the catalyst bed was then adjusted to the desired reaction temperature before the introduction of CCl_4 and H_2 mixture. For all the runs the CCl_4 (liquid) and the H_2 (gas) flow rate were set at 0.01 ml/min and 23 cm^3/min, respectively, corresponding to a $CCl_4 : H_2$ molar ratio of 1 : 10. The reaction was carried out at temperatures between 90 and 150°C and at 1 atm. The product mixture was sampled periodically by the sampling valve connected to the on-line computerized GC.

For catalyst tests in the differential mode, the catalyst bed contained 5–40 mg of catalyst particles diluted in about 4 g of 40–60 mesh SiC particles. The testing procedure was the same as that in the integral mode. The $CCl_4 : H_2$ molar ratio was set constant at 1 : 10 and CCl_4 (liquid) and H_2 (gas) flow rates were set in the ranges of 0.01–0.03 ml/min and 23–69 cm^3/min, respectively. This corresponds to a total feed gas flow between 25.3 cm^3/min and 75.9 cm^3/min and a residence time between 2.0 and 5.9 s. The reaction temperature was varied between 100 and 140°C. The CCl_4 conversion for each run was maintained between 1 and 5% to ensure differential conditions within the reactor by changing the catalyst weight and varying the flow rate of the feed gases. Under these testing conditions, no appreciable catalyst deactivation was observed for the catalysts during the first 2–3 h of reaction when GC data were collected except for the $PdCl_2$–Bu_4NCl/SiO_2 base catalyst, for which fresh catalyst sample was charged to the reactor at each temperature and GC data were collected during the first hour on stream when the activity of the catalyst was stable. One of the catalysts was also tested in a powder form (by crushing the 40–60 mesh catalyst particles and diluting with powder of the same SiO_2 support) under identical reaction conditions to examine the effect of pore diffusion inside the catalyst particles.

Product Analysis by GC-MS

Liquid products were trapped in a glass U-tube (i.d., 10 mm; height, 150 mm) positioned between the reactor outlet and the outlet transfer line and connected by means of 1/8″ stainless steel tubes and rubber plugs. The U-tube was half immersed into a Dewar flask partially filled with liquid N_2 to just below the bottom of the tube and the top of the Dewar was covered with aluminum foil. Cold gaseous N_2 inside the Dewar provided sufficient cooling for liquifying, but not for solidifying, HCl formed in hydrodechlorination. After passing the reaction mixture through the trap for 3 h, the trap was disconnected from the reactor and slowly warmed to ambient temperature to remove HCl and other substances with boiling points below room temperature. The residual liquid was transferred to a vial containing solid NaOH and dried $CuCl_2$ (HCl and water scavengers, respectively), and stored overnight before GC-MS analysis. GC-MS analysis was performed on a TRIO-1 GC-MS (Fison Instruments) equipped with an HP 5890 GC (Hewlett-Packard) with 15-m × 0.32-mm i.d. capillary column covered by 1 μm DB-1 stationary phase (J & B Scientific). The resulting mass spectrometry patterns were compared to a data base library included in the Fison Instruments software.

Pore Volume Measurements

A supported molten salts catalyst is characterized by its liquid loading, defined as the fraction of the total pore volume of a carrier occupied by the melt. The pore volumes of all catalysts were measured with a pulse technique using Micromeritics Pulse Chemisorb 2700. Both the carrier gas (95% N_2–5% He mixture) and the adsorbing gas (pure N_2) were purified by passing through gas driers and oxygen traps. First, the nitrogen gas was condensed into the catalyst pores at liquid nitrogen temperature; then it was allowed to reach equilibrium with the flowing N_2–He mixed carrier gas at a flow rate of 16 cm^3/min to achieve 95% N_2 saturation. The condensed nitrogen inside the pores was then allowed to evaporate at room temperature in the flowing N_2–He mixed carrier gas. The amount of nitrogen desorbed was measured by a thermal conductivity detector. The same experiment was also performed on a pure silica sample for comparison. Each experiment was performed at least two times to check for data consistency and the averaged value was reported.

Transmission Electron Microscopy (TEM)

A Hitachi H-600 electron microscope operating in both bright and dark field mode with an accelerating voltage of 100 kV was employed to perform TEM measurements. To avoid catalyst contamination by SiC and quartz wool particles and to facilitate catalysts removal from a reactor, samples of molten salt catalysts (A)–(E) for TEM measurements were prepared without SiC diluent, with glass wool plugs instead of quartz wool and in a glass tube (i.d., 8 mm) instead of a stainless steel reactor. A batch of 40–60 mesh SiC used as a preheater (~5 cm long) was positioned upstream and separated from the catalysts by a glass wool

plug. After purging with He as described above, the catalysts were treated with $H_2:CCl_4$ mixture (10:1) at 130°C for 36 h and then cooled in He flow to room temperature and removed from the reactor. The catalysts were ground separately with an agate mortar and pestle, suspended in methanol, and placed on a copper grid (400 mesh). For all catalyst samples, at least three different areas on the same grid were measured.

RESULTS

Characterization

A total of five silica-supported $PdCl_2$-containing molten salt catalysts were synthesized for this study, and tetrabutylammonium chloride was used as the molten medium in all cases. The organic salt tetrabutylammonium chloride has a relatively low melting point (about 42°C). Simple melting tests showed that after dissolving $PdCl_2$, $CoCl_2$, and $CuCl_2$ in Bu_4NCl in the same mole ratios as for the supported catalysts, the resulting mixture had a melting point of about 60°C.

Table 1 shows the compositions for all five catalysts in weight percentage; the numbers in parentheses indicate the molar ratios between the chloride salts. Note that the first four catalysts were prepared with about the same $PdCl_2$ loading (3.2 wt%) and also roughly the same total salt loading such that the liquid loading in these catalysts could be kept almost equal and the effects of doping $CoCl_2$ and $CuCl_2$ could be investigated. The $PdCl_2$ content of the last catalyst was only 1/4 of that of the other four catalyst and its total salt loading was about the same as the others.

Results from N_2 pore volume measurements showed that pure SiO_2 had a pore volume of 1.351 ± 0.005 cm^3/g (averaged over three runs), which agrees with the supplier's specification. The measured values of the pore volume for the silica-supported molten salt catalysts are in the narrow range 1.12–1.19 cm^3/g SiO_2 apparently because of the similarity in their total salt loadings, as shown in Table 1. The values for the liquid loading were calculated based on the pore volume data and they were in the range of 11.8–16.6%. However, the numbers should be regarded strictly as the "solid loading" since the measurements were performed at near liquid nitrogen temperature (77 K), which was much below the melting point of the chloride salt mixture. These low values of liquid loading are anticipated because the total salt loadings are relatively low.

A straight cylindrical pore with open ends was applied as an ideal model in calculations of the catalyst liquid loadings based on their salt loadings, densities of each chloride salt, and the pore volume and the average pore radius of the silica support. The model also assumed that the volume of each salt component is additive upon mixing and that the salt mixture is uniformly distributed on the inner wall of the cylindrical pore. The calculated values are also listed in Table 1 for comparison with the measured values. In all cases, the calculated value for liquid loading closely matched that from experiment, indicating that the catalysts were well prepared and most of the chloride salts were deposited inside the silica pores instead of being deposited on the exterior of the silica particles. The small differences between the two sets of values could be due to nonideality of the pores or experimental error. The average molten salt film thicknesses, also calculated from this model, are listed in the last column of Table 1. A very thin film (9–11 Å) of chloride salts was coated on the pore walls in the silica, corresponding to only a few molecular layers.

TEM measurements were performed to determine if Pd particles were forming in the supported catalysts during CCl_4 hydrodechlorination and, if they did, the uniformity of their distribution. It was shown that bright field images of all catalysts, which had performed CCl_4 hydrodechlorination for 36 h before measurements, had dark images

TABLE 1

Composition and Properties of Silica-Supported Molten Salt Catalysts

Catalyst	Composition (mole ratio)	Total salt wt%	Pore volume (cm^3/g cat)	Liquid loading		Film thickness (Å)
				Measured	Calculated	
	SiO_2	0	1.351	0	0	0
A	3.25% $PdCl_2$–18.94% Bu_4NCl/SiO_2 (1:3.7)	22.2	1.147	15.1	15.8	10.3
B	3.25% $PdCl_2$–2.39% $CoCl_2$–16.47% Bu_4NCl/SiO_2 (1:1:3.2)	22.1	1.14	15.6	14.5	9.4
C	3.13% $PdCl_2$–2.39% $CuCl_2$–17.84% Bu_4NCl/SiO_2 (1:1:3.6)	23.4	1.126	16.6	16	10.5
D	3.21% $PdCl_2$–1.17% $CoCl_2$–1.21% $CuCl_2$–17.27% Bu_4NCl/SiO_2 (2:1:1:6.9)	22.9	1.152	14.7	15.3	9.9
E	0.82% $PdCl_2$–1.20% $CoCl_2$–1.26% $CuCl_2$–17.73% Bu_4NCl/SiO_2 (1:2:2:13.9)	21	1.191	11.8	14.2	9.2

(particles); in dark field, almost all particles remained dark, indicating that these particles were not metallic Pd. For three of the five catalysts treated for 36 h, samples of $PdCl_2$–Bu_4NCl/SiO_2 (A), $PdCl_2$–$CuCl_2$–Bu_4NCl/SiO_2 (C), and $PdCl_2$–$CoCl_2$–$CuCl_2$–Bu_4NCl/SiO_2 (D) catalysts contained 1–2 bright spots per 300–900 nm^2. They looked like metallic spots of 5–15 nm in diameter (by considering the particles spherical), partially covering larger dark particles. Catalysts B and E did not possess any metallic particles.

CCl_4 Hydrodechlorination

For the purpose of direct comparison between all catalysts, the amount of catalyst loaded into the reactor tube was kept at about 0.6 g for all the runs in the integral mode. The CCl_4 conversion was calculated as the ratio of carbon in the products to the total amount of carbon, including unreacted CCl_4. Figure 2a shows the test results as CCl_4 conversion versus reaction time for the first four catalysts listed in Table 1, i.e., $PdCl_2$–$(C_4H_9)_4NCl/SiO_2$, $PdCl_2$–$CoCl_2$–$(C_4H_9)_4NCl/SiO_2$, $PdCl_2$–$CuCl_2$–$(C_4H_9)_4NCl/SiO_2$, and $PdCl_2$–$CoCl_2$–$CuCl_2$–$(C_4H_9)_4NCl/SiO_2$ (D, with 3.21 wt% $PdCl_2$). The reaction temperature was 130°C with other parameters as described above. The $PdCl_2$–$(C_4H_9)_4NCl/SiO_2$ catalyst initially showed a CCl_4 conversion of about 85%, but its conversion dropped appreciably in the next 15 h. With addition of $CoCl_2$ the initial CCl_4 conversion increased to 99.3% and deactivation occurred at a much slower rate than with the $PdCl_2$–$(C_4H_9)_4NCl/SiO_2$ catalyst. The results for both $PdCl_2$–$CuCl_2$–$(C_4H_9)_4NCl/SiO_2$ and $PdCl_2$–$CoCl_2$–$CuCl_2$–$(C_4H_9)_4NCl/SiO_2$ (D) showed striking stability for CCl_4 conversion over a period of more than 50 h. The initial CCl_4 conversions were 94.5 and 99.5% for the two catalysts, respectively. The addition of $CuCl_2$ appeared to prolong significantly the life of both the $PdCl_2$–$(C_4H_9)_4NCl/SiO_2$ and $PdCl_2$–$CoCl_2$–$(C_4H_9)_4NCl/SiO_2$ catalysts. The initial CCl_4 conversion was between 60 and 85% at 110°C for all four catalysts.

Figure 2b compares the results of CCl_4 conversion versus time at 130°C for two $PdCl_2$–$CoCl_2$–$CuCl_2$–$(C_4H_9)_4NCl/SiO_2$ catalysts. The second catalyst (E, with 0.82 wt% $PdCl_2$) contains only 25% $PdCl_2$ as in the first catalyst (D) (see Table 1) but has the same amounts of $CoCl_2$, $CuCl_2$, and $(C_4H_9)_4NCl$. While the first catalyst showed excellent stability for CCl_4 conversion, the second catalyst had an initial CCl_4 conversion of 73% and was stable for the first 8 h. It was deactivated gradually over a period of about 23 h down to a CCl_4 conversion of 57%. The decrease in the initial CCl_4 conversion is expected since $PdCl_2$ is the only active chloride salt in the catalyst. This was proven by performing two separate experiments with a $CoCl_2$–$(C_4H_9)_4NCl/SiO_2$ and a $CuCl_2$–$(C_4H_9)_4NCl/SiO_2$ catalyst, both of which showed near zero CCl_4 conversion under the same reaction conditions. Even with such a small amount of $PdCl_2$, the deactivation trend for the second catalyst was much more gradual than that of the $PdCl_2$–$(C_4H_9)_4NCl/SiO_2$ base catalyst shown in Fig. 2a. This also indicates the stabilizing effects of both $CoCl_2$ and $CuCl_2$ on the $PdCl_2$–$(C_4H_9)_4NCl/SiO_2$ base catalyst.

In Figs. 3a and 3b, hydrocarbon and chlorocarbon product mole percents are plotted against time for the four catalysts shown previously in Fig. 2a. Product distribution for all four catalysts are also presented in Fig. 4a—after 2 h on stream—and in Fig. 4b—near the end of the reaction period. Because the catalysts can be separated into two groups based on their longevity, namely A–B and C–D, data in Fig. 4b represent product distributions for catalysts A and B after about 12 h on stream and for catalysts C and D after 47 h, with corresponding CCl_4 conversions of 71, 95.2, 92, and 97%. For the $PdCl_2$–$(C_4H_9)_4NCl/SiO_2$ base catalyst, the products contain mostly C_1–C_5 paraffins and C_2–C_4 olefins, with variable amounts of CH_2Cl_2, $CHCl_3$, $CHClCCl_2$, and CCl_2CCl_2. In addition to those products detected by GC, GC-MS analysis of condensed products showed the presence of 1,1,3,4-tetrachloro-, pentachloro-, and hexachlorobutadiene, and confirmed the absence of CCl_3CCl_3. Because chlorinated butadienes were present in trace amounts, they were not taken into account for calculations of CCl_4 conversion and product distribution. The hydrocarbon percentage remained roughly constant between 66 and 78% during the course of the reaction, while product distribution was gradually changing, with CH_4, CH_2Cl_2, and $CHCl_3$ decreasing and C_2H_4, C_{3+}-alkanes and $C_2H_xCl_y$ ($CHClCCl_2 + CCl_2CCl_2$) increasing.

With the addition of $CoCl_2$ the initial hydrocarbon percentage was increased by about 7% and it decreased gradually with reaction time. The product distribution of hydrocarbons and chlorocarbons was different from that of the $PdCl_2$–$(C_4H_9)_4NCl/SiO_2$ base catalyst. Addition of $CoCl_2$ led to an increase in hydrocarbon products, especially in C_2H_6 and C_{3+}–alkanes, and to a decrease in chlorocarbon products. During the reaction period, the percentage of CH_4, C_2H_6, CH_2Cl_2, and $C_2H_xCl_y$ decreased, while $CHCl_3$, C_2H_4, and C_{3+}-alkanes increased. For both catalysts A and B, the CH_2Cl_2 yield was always smaller than that of $CHCl_3$.

When $CuCl_2$ or both $CoCl_2$ and $CuCl_2$ was added to the base catalyst, the hydrocarbon yield was decreased and the chlorocarbon yield increased. The main change in the product distribution with $CuCl_2$ addition was an increase in both CH_2Cl_2 and $CHCl_3$ and a decrease in CCl_2CCl_2 and $CHClCCl_2$. At the end of the reaction period, CH_2Cl_2 and $CHCl_3$ became the major products of CCl_4 hydrodechlorination for catalysts C and D, with CH_2Cl_2 yield higher than that of $CHCl_3$. Catalysts without Pd but with the same concentration of other salts did not show any substantial activity in CCl_4 hydrodechlorination.

The rates of CCl_4 conversion, expressed as specific activity (g mole CCl_4 converted per gram catalyst per minute) and turnover frequency (TOF, mole CCl_4 converted per

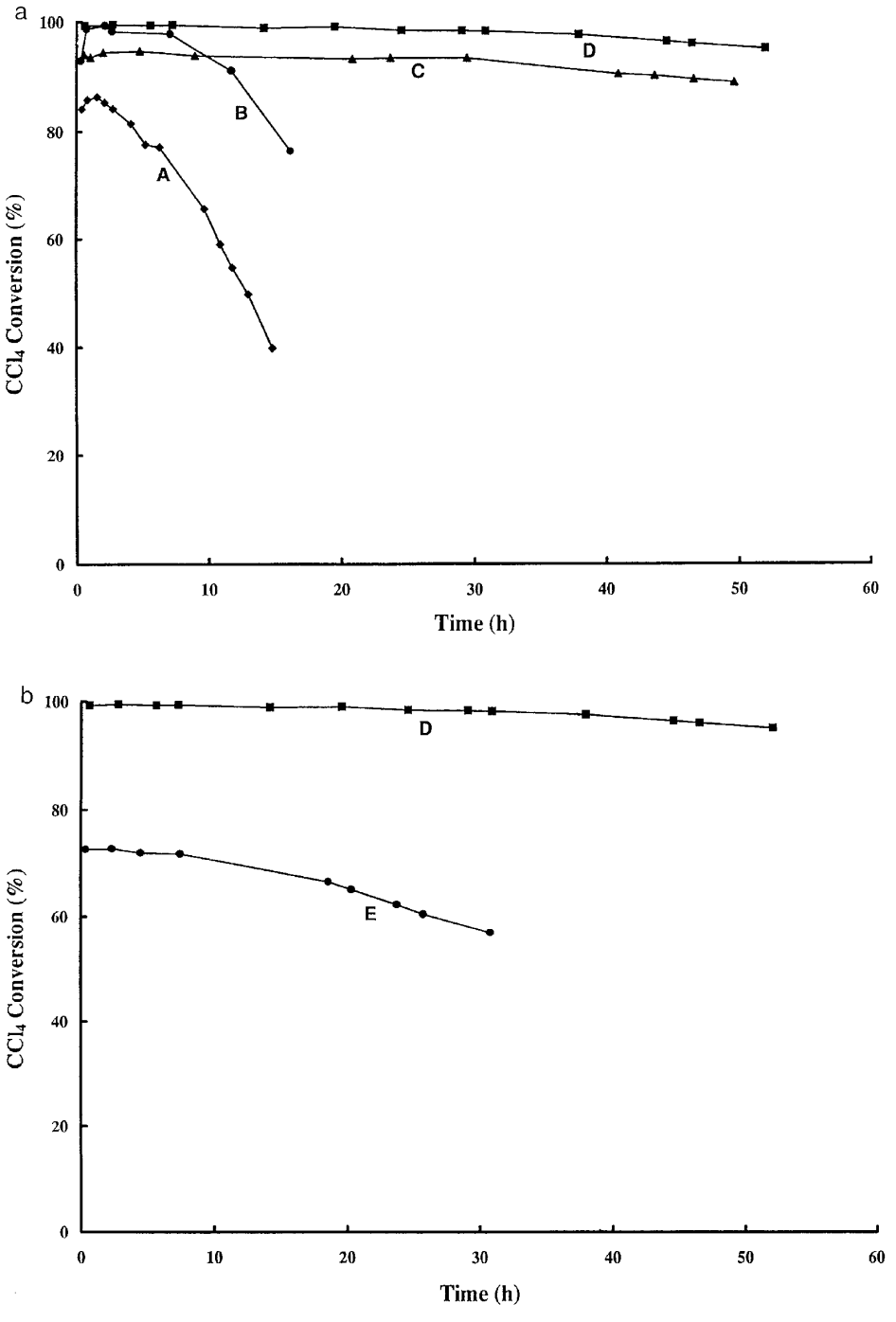

FIG. 2. (a) Comparison of CCl_4 conversion versus time for four $PdCl_2$-containing molten salt catalysts: (A) $PdCl_2$–$(C_4H_9)_4NCl/SiO_2$, (B) $PdCl_2$–$CoCl_2$–$(C_4H_9)_4NCl/SiO_2$, (C) $PdCl_2$–$CuCl_2$–$(C_4H_9)_4NCl/SiO_2$, (D) $PdCl_2$–$CoCl_2$–$CuCl_2$–$(C_4H_9)_4NCl/SiO_2$. The reaction was carried out at 130°C and 1 atm with a CCl_4 flow rate of 0.01 ml/min and a $CCl_4 : H_2$ molar ratio of 1 : 10. (b) Comparison of CCl_4 coversion versus time for two $PdCl_2$–$CoCl_2$–$CuCl_2$–$(C_4H_9)_4NCl/SiO_2$ molten salt catalysts. Catalyst (D) contains 3.21 wt% $PdCl_2$ and Catalyst (E) 0.82 wt% $PdCl_2$. The reaction conditions were the same as in (a).

mole $PdCl_2$ per second) are presented and fitted with the Arrhenius equation in Fig. 5 for the $PdCl_2$–$(C_4H_9)_4NCl/SiO_2$, $PdCl_2$–$CoCl_2$–$(C_4H_9)_4NCl/SiO_2$, and $PdCl_2$–$CuCl_2$–$(C_4H_9)_4NCl/SiO_2$ catalysts. For computational purposes, it was assumed that $PdCl_2$ was the only active center for the hydrodechlorination of CCl_4 and that all $PdCl_2$ molecules in the molten salt liquid phase were accessible for the reaction. The data showed a similar temperature dependency of the catalytic activity for the $PdCl_2$–$(C_4H_9)_4NCl/SiO_2$ and the $PdCl_2$–$CuCl_2$–$(C_4H_9)_4NCl/SiO_2$ catalysts, but the data

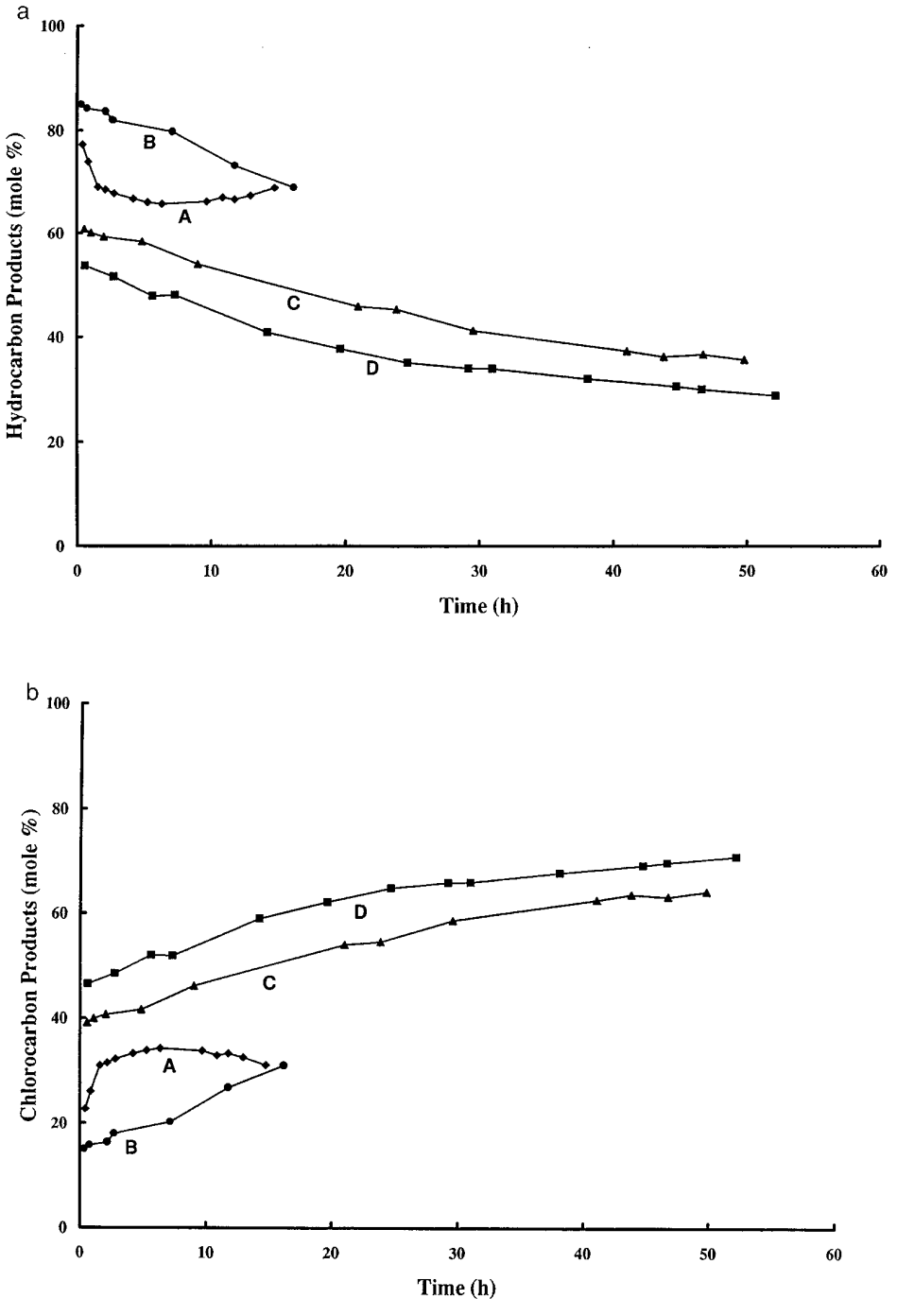

FIG. 3. (a) Comparison of hydrocarbon mole percent in products versus time for four $PdCl_2$-containing molten salt catalysts: (A) $PdCl_2$–$(C_4H_9)_4NCl/SiO_2$, (B) $PdCl_2$–$CoCl_2$–$(C_4H_9)_4NCl/SiO_2$, (C) $PdCl_2$–$CuCl_2$–$(C_4H_9)_4NCl/SiO_2$, (D) $PdCl_2$–$CoCl_2$–$CuCl_2$–$(C_4H_9)_4NCl/SiO_2$. The reaction was carried out at 130°C and 1 atm with a CCl_4 flow rate of 0.01 ml/min and a $CCl_4 : H_2$ molar ratio of 1 : 10. (b) Comparison of chlorocarbon mole percent in products versus time for the same four $PdCl_2$-containing molten salt catalysts (A)–(D). The reaction conditions were the same as in (a).

for the $PdCl_2$–$CoCl_2$–$(C_4H_9)_4NCl/SiO_2$ catalyst exhibited a stronger temperature dependency than the other two catalysts. The measured apparent activation energies for the three catalysts were 16.49, 15.84, and 22.78 kcal/mol, respectively.

For the two $PdCl_2$–$CoCl_2$–$CuCl_2$–$(C_4H_9)_4NCl/SiO_2$ catalysts, the Arrhenius plots for the rates of CCl_4 conversion in specific activities and turnover frequencies are shown in Fig. 6. The rate data indicated that although the specific activities for the first $PdCl_2$–$CoCl_2$–$CuCl_2$–

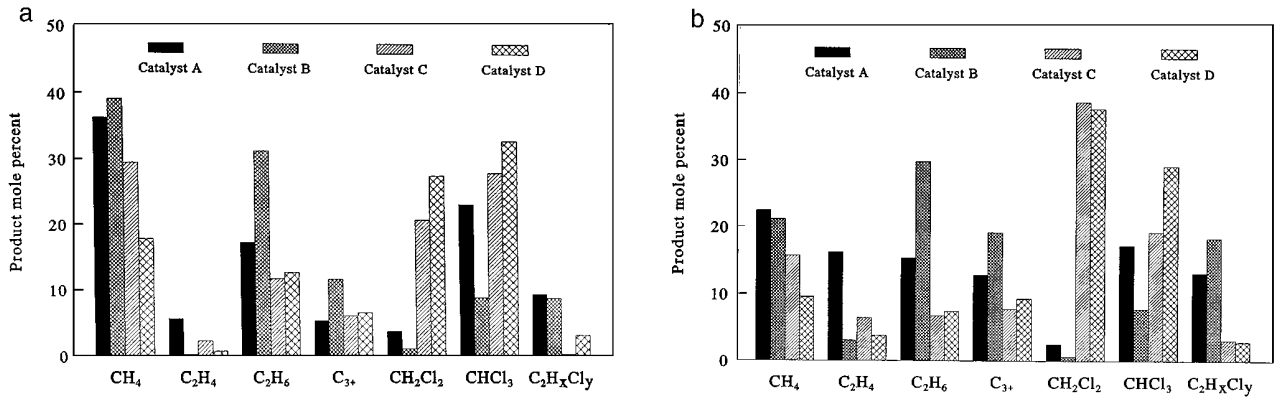

FIG. 4. (a) Comparison of total product distribution at 2 h into experiment for four molten salt catalysts: (A) $PdCl_2$–$(C_4H_9)_4NCl/SiO_2$, (B) $PdCl_2$–$CoCl_2$–$(C_4H_9)_4NCl/SiO_2$, (C) $PdCl_2$–$CuCl_2$–$(C_4H_9)_4NCl/SiO_2$, (D) $PdCl_2$–$CoCl_2$–$CuCl_2$–$(C_4H_9)_4NCl/SiO_2$. (b) Comparison of total product distribution near the end of the reaction period for the same four $PdCl_2$-containing molten salt catalysts (A)–(D) at the following time into experiment (CCl_4 conversion): (A) 11 h, 71%; (B) 11 h, 95.2%; (C) 47 h, 92%; and (D) 97%. The reaction conditions were the same as in (a).

$(C_4H_9)_4NCl/SiO_2$ catalyst (containing 3.21 wt% $PdCl_2$) were much higher than those for the second $PdCl_2$–$CoCl_2$–$CuCl_2$–$(C_4H_9)_4NCl/SiO_2$ catalyst (containing 0.82 wt% $PdCl_2$), the turnover frequencies for the second catalyst were somewhat higher than the first. There was also a greater temperature dependency for the second catalyst than that for the first. The measured apparent activation energies for the two catalysts were 15.65 and 17.91 kcal/mol, respectively.

The kinetic data for all five silica-supported molten salt catalysts were obtained from the Arrhenius plots previously shown in Figs. 5 and 6, and the values are presented in Table 2. The preexponential factors were calculated based on both the specific activity and the turnover frequency, and the apparent activation energies were obtained from the slopes of the Arrhenius plots. The preexponential factors and the activation energy for the $PdCl_2$–$CoCl_2$–Bu_4NCl/SiO_2 catalyst were the highest and those for the $PdCl_2$–Bu_4NCl/SiO_2, $PdCl_2$–$CuCl_2$–Bu_4NCl/SiO_2, and the first $PdCl_2$–$CoCl_2$–$CuCl_2$–Bu_4NCl/SiO_2 catalyst (D) were comparable. The values of kinetic data for the second $PdCl_2$–$CoCl_2$–$CuCl_2$–Bu_4NCl/SiO_2 catalyst (E) were somewhat higher than those of the three catalysts but lower than those of the $PdCl_2$–$CoCl_2$–Bu_4NCl/SiO_2 catalyst. The result

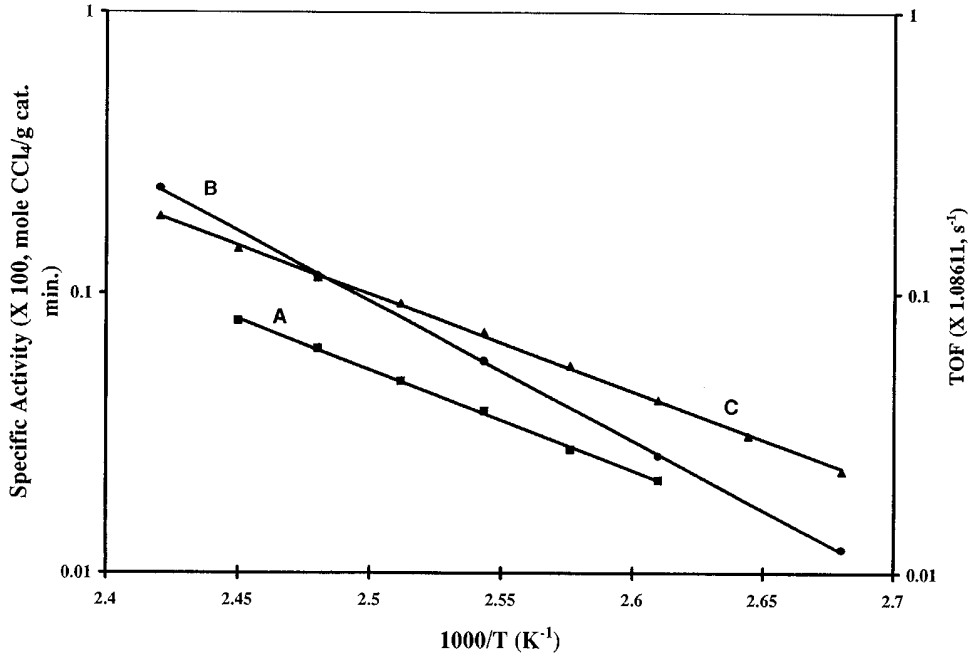

FIG. 5. An Arrhenius plot of the specific activity and the turnover frequency for three catalysts: (A) $PdCl_2$–Bu_4NCl/SiO_2, (B) $PdCl_2$–$CoCl_2$–Bu_4NCl/SiO_2, and (C) $PdCl_2$–$CuCl_2$–Bu_4NCl/SiO_2.

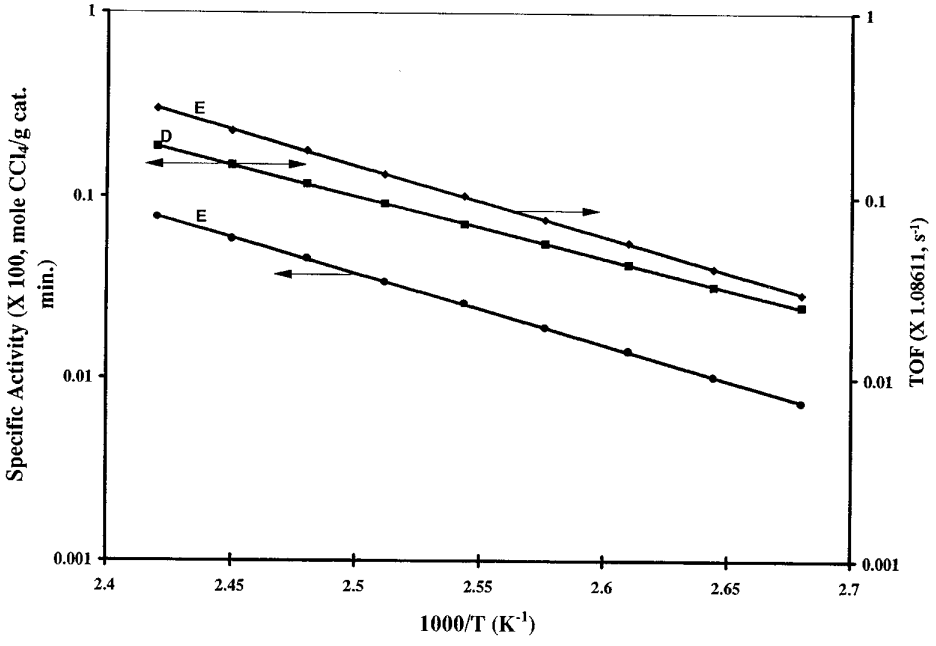

FIG. 6. An Arrhenius plot of the specific activity and the turnover frequency for two catalysts: (D) 3.21% $PdCl_2$–1.17% $CoCl_2$–1.21% $CuCl_2$–17.27% Bu_4NCl/SiO_2 and (E) 0.82% $PdCl_2$–1.20% $CoCl_2$–1.26% $CuCl_2$–17.73% Bu_4NCl/SiO_2.

from the test on a powder sample of the $PdCl_2$–$CuCl_2$–Bu_4NCl/SiO_2 catalyst indicated that the specific activities and turnover frequencies were increased by only 10% over the 40–60 mesh particle sample and the slopes from the Arrhenius plots were virtually unchanged. Therefore, pore diffusion through the catalyst particles was relatively insignificant and the measured apparent activation energies were essentially the intrinsic activation energies. The estimated errors for the measured activation energies were within ±0.5 kcal/mol.

DISCUSSION

Mechanisms for Hydrodechlorination

Hydrodechlorination of CCl_4 in the presence of H_2 gas over Ni/Y zeolites catalysts has been proposed to follow the sequential free radical mechanism with formation of $\cdot CCl_3$, $\cdot CHCl_2$, $\cdot CH_2Cl$, and $\cdot CH_3$ radicals in sequential steps in the gas phase near the active catalytic sites at a relatively high temperature (370°C) and formation of C_2-chlorocarbons proceeds through termination reactions of the adsorbed free radicals at the catalytic sites for conventional supported catalysts (2). However, it is unclear exactly what mechanism the reaction follows at relatively low reaction temperatures (below 150°C) for our supported molten salt catalysts. Under these conditions, the gaseous free radical mechanism seems unlikely but the adsorbed radical scenario (1) is more reasonable. The adsorbed radical should be in a much lower energy state than the gaseous free radical; therefore, it can be generated at relatively low reaction temperatures.

For our molten salts, the active sites for activation of molecular hydrogen and for adsorbed radicals or

TABLE 2

Kinetic Data for Five Silica-Supported Molten Salt Catalysts

Catalyst	Composition	A_1[a] (mol g cat^{-1} min^{-1})	A_2[b] (s^{-1})	E_a (kcal/mol)
A	$PdCl_2$–Bu_4NCl/SiO_2	5.47×10^5	4.97×10^7	16.49
B	$PdCl_2$–$CoCl_2$–Bu_4NCl/SiO_2	2.64×10^9	2.40×10^{11}	22.78
C	$PdCl_2$–$CuCl_2$–Bu_4NCl/SiO_2	4.47×10^5	4.22×10^7	15.84
D	$PdCl_2$–$CoCl_2$–$CuCl_2$–Bu_4NCl/SiO_2[c]	3.56×10^5	3.28×10^7	15.65
E	$PdCl_2$–$CoCl_2$–$CuCl_2$–Bu_4NCl/SiO_4[d]	2.29×10^6	8.33×10^8	17.91

[a] Preexponential factor calculated based on specific activities shown in Figs. 5 and 6.
[b] Preexponential factor calculated based on turnover frequencies shown in Figs. 5 and 6.
[c] The catalyst contained 3.21% $PdCl_2$, 1.17% $CoCl_2$, 1.21% $CuCl_2$, and 17.27% Bu_4NCl by weight.
[d] The catalyst contained 0.82% $PdCl_2$, 1.20% $CoCl_2$, 1.26% $CuCl_2$, and 17.73% Bu_4NCl by weight.

intermediates may take the form of either fine, suspended Pd(0) particles or dissolved Pd(II) chloride complex in the melt or both; they are present both on the surface and in the bulk of the liquid thin film. According to the data listed in Table 1, the film thickness of the molten layer is only a few molecules. Diffusion of CCl_4 and H_2 through the thin film should be unrestricted, and all Pd-containing catalytic sites should be accessible to the two reactants. The thickness of the thin film can be increased by increasing the molten salt loading. The $PdCl_2$ active site density within the catalyst pores can also be increased by preparing a catalyst with higher $PdCl_2$ loading.

Another possibility is a nonradical mechanism for the hydrodechlorination with activation of CCl_4 as proposed by Drago and co-workers (4) for silica-gel–Lewis acid sites by generation of a carbenium-like species such as silica-gel–$AlCl_3^-$ CCl_3^+, followed by a nucleophilic attack on carbon by hydrogen activated by Pd species. Activation of CCl_4 at acidic sites with generation of the carbenium-like species can be performed to some extent in our catalytic environment by Lewis acids such as Co(II) and Cu(II) and can be followed by a nucleophilic attack on carbon by hydrogen activated by elemental Pd or Pd(II) complexes in supported molten salts. The reductive capability of the activated hydrogen, in the form of atomic hydrogen associated with either Pd(0) or Pd(II) complexes or both, seems to be influenced by the Pd environment in the presence of anions such as $CoCl_4^{2-}$ and $CuCl_4^{2-}$, as reflected from the final product distribution indicating the extent of CCl_4 hydrodechlorination. The actual hydrodechlorination mechanism for CCl_4 could be determined by the final composition of Pd active sites, and there is a possibility of coexistence of the two reaction mechanisms.

Reaction Products

For the $PdCl_2$–$(C_4H_9)_4NCl/SiO_2$ catalyst, product distribution is different from any one of the two types of SG–$AlCl_2$–$PdCl_2$ catalysts (4). The latter produced mostly $CHCl_3$ or mostly hydrocarbons, in contrast to the former, which produced, in addition to both $CHCl_3$ and C_1–C_4 hydrocarbons, CH_2Cl_2 and substantial amounts of chlorinated ethylenes CCl_2CCl_2 and $CHClCCl_2$ and trace amounts of 1,1,3,4-tetrachloro-, pentachloro-, and hexachlorobutadiene. The formation of these chloroalkenes can proceed through the following dimerization, hydrogenation, and dehydrochlorination reactions:

$$2 \cdot CCl_3 \Rightarrow CCl_3CCl_3 \quad [A]$$

$$CCl_3CCl_3 + H_2 \Rightarrow CCl_2CCl_2 + 2HCl \quad [B]$$

$$2 \cdot CCl_3 + H_2 \Rightarrow 2CHCl_3 \text{ or } 2{:}CCl_2 + 2HCl \quad [C]$$

$$2{:}CCl_2 \Rightarrow CCl_2CCl_2 \quad [D]$$

$${:}CCl_2 + H_2 \Rightarrow CH_2Cl_2 \quad [E]$$

$$CCl_2CCl_2 + H_2 \Rightarrow CHClCCl_2 + HCl. \quad [F]$$

Formation of chlorinated butadienes could proceed further through similar reduction and dimerization reactions of C_2-chlorocarbons. Further chain growth could lead to C_{6+}-chloroalkenes and chloroalkanes and to formation of polychlorinated hydrocarbons or coke-like species.

Reactions [A]–[D] were written by analogy with those proposed by Assher and Vofsi (20), where both CCl_3CCl_3 and CCl_2CCl_2 but not C_{3+}-chlorocarbons were formed in reduction of CCl_4 by Fe(II) in acetonitrile, and both $\cdot CCl_3$ and $:CCl_2$ were trapped by cyclohexene (20). In contrast to that reported in this article, we did not observe CCl_3CCl_3. That means that $\cdot CCl_3$ coupling does not proceed in a hydrogen-rich environment (feed mole ratio $H_2 : CCl_4 = 10 : 1$) and $PdCl_2$–$(C_4H_9)_4NCl$ molten salt medium, or CCl_3CCl_3 was converted rapidly to CCl_2CCl_2 through dechlorination followed by chlorine reaction with hydrogen. A nonionic mechanism was proposed for such dechlorination reactions of gem-chloroalkanes in the presence of H_2 over Pd/SiO_2 at 300°C (21).

Our results on reaction products (see Figs. 3a and 3b, 4a and 4b) indicate that the $PdCl_2$–$CoCl_2$–$(C_4H_9)_4NCl/SiO_2$ catalyst leads to more hydrocarbons and fewer C_1-chlorocarbons than the base catalyst but the $CuCl_2$-containing catalysts give less hydrocarbons and more CH_2Cl_2 and $CHCl_3$. One can attribute these variations in product distribution upon addition of promoters to the changes in hydrogenation efficiency of these catalysts. It seems that the hydrogenation capability of the base catalyst improves with the addition of $CoCl_2$ but is somewhat limited with the addition of $CuCl_2$. However, the observation of less $C_2H_xCl_y$ formation for the $CuCl_2$-containing catalysts than the $PdCl_2$–$CoCl_2$–$(C_4H_9)_4NCl/SiO_2$ catalyst and the base catalyst (see Figs. 4a and 4b) suggests that the presence of $CuCl_2$ can suppress the coupling reaction of the adsorbed C_1-radicals and probably the formation of polychlorocarbons (coke precursors) at the Pd-containing catalytic sites.

Deactivation of the Base Catalyst

The deactivation of the $PdCl_2$–$(C_4H_9)_4Cl/SiO_2$ molten salt catalyst for hydrodechlorination of CCl_4 in a hydrogen-rich environment may be caused by one or more factors. In an attempt to pinpoint the exact cause, we propose, with supporting evidence, several possible deactivation mechanisms including: (a) partial reduction of $PdCl_2$ to fine metallic Pd particles by the excess hydrogen present and subsequent agglomeration of the Pd metal; (b) formation of chlorinated oligomers/polymers, coke, PdC, or carbide-like $PdCH_x$ species, blocking the active catalytic sites; (c) accumulation of chloride ions inside the catalyst pores, possibly replacing the surface hydroxyl group around the pore walls; (d) slow evaporation or decomposition of tetrabutylammonium chloride over time.

In a separate experiment, passing hydrogen gas through a $PdCl_2$–$(C_4H_9)_4NCl$ melt at about 130°C indeed resulted

in formation of some fine black Pd particles. However, most of the $PdCl_2$ (approximately 83%) was still dissolved and remained in the $(C_4H_9)_4NCl$ melt after removal of the Pd particles and upon further bubbling H_2 or H_2-CCl_4 mixture (about 16 vol% of CCl_4). A continuous bubbling of the H_2–CCl_4 mixture through the melt resulted in conversion of about 14% of CCl_4 to C_{1-3}-hydrocarbons and $CHCl_3$. The observed low activity of the unsupported catalyst solution compared to that supported on SiO_2 may be due to better interaction of reactant gases with the thin layer of catalytic solution having a large interfacial area in the case of supported catalyst. TEM measurements of all catalysts performed after CCl_4 hydrodechlorination for 36 h, showed that some metallic particle formation occurred in the catalysts A, C, and D and was absent in the catalysts B and E. The length of the experiment allowed deactivation of catalysts A, B, and E, while catalysts C and D still showed high CCl_4 conversion (Figs. 2a and 2b). Because the catalysts A–D have the same Pd concentration of 2 wt%, usually visible in TEM pictures of catalysts without molten salts when Pd is in metallic state (17), it was concluded that in general the Pd(0) agglomeration into metallic particles large enough to be detected by TEM was not the major cause of deactivation of the molten salt catalysts. Absence of metallic particles on the TEM micrographs of the catalyst E while they are present on the micrographs of the catalyst D could be partially due to lower Pd concentration.

Detection of tetra-, penta-, and hexachlorobutadienes in the gas phase can be considered as a direct evidence of oligomerization of CCl_4 around catalytic active sites. It is highly possible that these oligomers would undergo further transformation to form C_{6+}-chlorocarbons (coke precursors) and chlorinated coke, which are not volatile at the reaction temperature of 130°C and would block the active sites.

The accumulation of chloride ions by means of exchange of Cl^- with the surface hydroxyl groups in the silica support cannot be confirmed experimentally in the present study, but it is likely to occur at 130°C in the presence of excess gaseous HCl. However, it is unclear how the accumulation of Cl^- will affect the catalytic activity of the molten salts, although strong correlation between Cl^- accumulation and deactivation of conventional Pt/Al_2O_3 catalysts has been established in two separate studies (18), possibly due to the influence of Cl^- on the rate of agglomeration of the Pt particles. Tetrabutylammonium chloride begins to decompose at temperatures higher than about 170°C, as shown by a blank experiment with only $(C_4H_9)_4NCl/SiO_2$ in the reactor tube. 1-Butene was detected as one of the decomposition products by GC. Bubbling hydrogen through a melt of $(C_4H_9)_4NCl$ overnight also resulted in some evaporation. While it is possible that all these factors play a role in the deactivation of the $PdCl_2$–$(C_4H_9)_4NCl/SiO_2$ molten salt catalyst, it is most likely that the second factor is the main cause for catalyst deactivation, simply because of the observed promotional effects of $CoCl_2$ and $CuCl_2$. The increased stability of the catalysts accompanying addition of $CoCl_2$ and/or $CuCl_2$ could be due to conversion of excess $(C_4H_9)_4NCl$, after formation of $[(C_4H_9)_4N]_2Pd_2Cl_6$ (19), into ionic complexes with anions such as $CuCl_4^{2-}$, $CoCl_4^{2-}$, and $CuCl_3^-$, which interact with the Pd(II) active centers.

Promotional Effects of $CoCl_2$ and $CuCl_2$

The promotional effect of $CoCl_2$ to enhance the catalytic activity of the base $PdCl_2$–$(C_4H_9)_4NCl/SiO_2$ molten salt catalyst may be simply due to the fact that $CoCl_2$ is a sufficiently strong Lewis acid, which assists the breaking of the C–Cl bond in the CCl_4 molecule. The stabilizing effect of $CoCl_2$ on the base catalyst may be due to interaction between $CoCl_2$ or $[CoCl_4]^{2-}$ and the $PdCl_2$, possibly in the form of a planar complex with two Cl atoms bridging between a Pd(II) cation and a Co(II) cation:

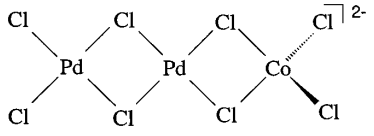

This interaction somehow maintains a more favorable hydrogenation environment around the $PdCl_2$-containing active centers, probably due to the electron withdrawing effect of the Co(II) cation through the bridging Cl atoms, which in turn causes a slightly more electron deficient Pd(II) environment. This modified Pd(II) active center would be more efficient in breaking the C–Cl and the H–H bond. This is consistent with the higher hydrocarbon and lower chlorocarbon contents in the reaction products for the $CoCl_2$-containing catalyst (see Catalyst B in Figs. 3 and 4), an indication of an improved hydrogenation capability. In addition, kinetics measurements on this catalyst indicated a much higher preexponential factor and a considerably higher activation energy than that of the base molten salt catalyst (see Table 2). The former parameter is an indication of an increase in collision frequency between the reactant molecules and the Pd(II) active centers while the latter is an indication of a change in the electronic environment around the active centers. Although there is a partial compensation effect from the two parameters in the Arrhenius equation, the resulting effect is an increase in the reaction rate for the $CoCl_2$-containing catalyst.

A similar interaction between $CuCl_2$ or $CuCl_3^-$ and $PdCl_2$-containing active centers may be prevalent as well. However, the stronger promotional effect by $CuCl_2$, especially in catalyst stability, may be more complex since CuCl can be formed as a stable compound during hydrodechlorination of CCl_4. Two interacting catalytic cycles (one for Pd(0)/Pd(II) and the other for Cu(II)/CuCl/Cu(0)) with seven possible steps are proposed to account for

the remarkable stabilizing effect of $CuCl_2$ on the $PdCl_2$–$(C_4H_9)_4NCl/SiO_2$ molten salt catalyst:

$$PdCl_2 + H_2 \Rightarrow Pd + 2HCl \quad [1]$$

$$2CuCl_2 + H_2 \Rightarrow 2CuCl + 2HCl \quad [2]$$

$$2CuCl_2 + Pd \Rightarrow 2CuCl + PdCl_2 \quad [3]$$

$$CuCl_2 + Pd \Rightarrow Cu + PdCl_2 \quad [4]$$

$$CuCl + CCl_4 \Rightarrow CuCl_2 + \cdot CCl_3 \quad [5]$$

$$Cu + CCl_4 \Rightarrow CuCl + \cdot CCl_3 \quad [6]$$

$$Pd + 2CCl_4 \Rightarrow PdCl_2 + 2\cdot CCl_3. \quad [7]$$

Although all the above reaction steps are thermodynamically feasible, it is not known if they all proceed under the reaction condition, and whether $Pd(0) \rightleftharpoons Pd(II)$ conversion is substantial for $CuCl_2$-containing catalysts. Rate constants for Steps [3], [4], and [7] in the proposed mechanism have to be large enough to ensure that deactivation of the catalyst does not proceed by Pd agglomeration. A reaction of CuCl with CCl_4 (Step [5]) performed in an acetonitrile solution containing LiCl at 22°C reached a quasi-equilibrium with as low as 1–5% conversion of Cu (I) into Cu(II) (20). At the higher temperature used in our case the equilibrium may be reached quickly, favoring the formation of Cu(II). Step [4] in the above mechanism also suggests the formation of Cu(0), which may interact with Pd(0) to form bimetallic Pd–Cu clusters. It is unlikely, because of the reactivity of Cu(0) with CCl_4 (Step [6], (22)), that Cu metallic particles would grow to a size detectable in TEM measurements. Similarity of TEM results for Pd- or Pd–Cu-containing catalysts A, C, and D showed that the presence of $CuCl_2$, unlike $CoCl_2$, did not eliminate the growth of metallic aggregates (most probably Pd(0)) to particles of a size detectable by TEM.

Although the rates of CCl_4 hydrodechlorination were increased with the addition of $CuCl_2$ (see Fig. 5), the significant effect of $CuCl_2$ was to stabilize the activity of the $PdCl_2$–Bu_4NCl/SiO_2 base catalyst (see Fig. 2a). In contrast to $CoCl_2$, the addition of $CuCl_2$ resulted in formation of more CH_2Cl_2 and $CHCl_3$ in the products (see Fig. 4), an indication of a reduced hydrogenation capability of the catalyst. Kinetics measurements on the $PdCl_2$–$CuCl_2$–Bu_4NCl/SiO_2 catalyst showed a somewhat lower value for the activation energy than that for the base catalyst, suggesting an electronic effect of $CuCl_2$ on the Pd(II) active center which is opposite to that caused by $CoCl_2$.

The measured reaction rates and activation energies for the $PdCl_2$–$CuCl_2$–Bu_4NCl/SiO_2 and the first $PdCl_2$–$CoCl_2$–$CuCl_2$–Bu_4NCl/SiO_2 catalyst were almost identical (see Fig. 5 and 6), but the activation energy for the second $PdCl_2$–$CoCl_2$–$CuCl_2$–Bu_4NCl/SiO_2 catalyst was somewhat higher than that of the $PdCl_2$–Bu_4NCl/SiO_2 base catalyst (see Table 2) yet lower than for the $PdCl_2$–$CoCl_2$–Bu_4NCl/SiO_2 catalyst. In the case of the second $PdCl_2$–$CoCl_2$–$CuCl_2$–Bu_4NCl/SiO_2 catalyst, $PdCl_2$ may be utilized more efficiently than the first catalyst because of the somewhat higher measured turnover frequencies (see Fig. 6). The fact that the measured reaction rates were approximately proportional to the $PdCl_2$ content in the supported molten salt catalysts may indicate that activation of molecular hydrogen is the rate limiting step for hydrodechlorination of CCl_4. Furthermore, the fact that the addition of $CuCl_2$ or $CoCl_2$ alters the product distribution toward CH_2Cl_2 and $CHCl_3$ or toward hydrocarbons, respectively, suggests the possibility of modifying or even controlling the selectivity of a certain desired product by doping one or more appropriate promoters.

CONCLUSIONS

Our results from five silica-supported $PdCl_2$-containing molten salt catalysts with $CoCl_2$ or $CuCl_2$ or both promoters, i.e., $PdCl_2$–$(C_4H_9)_4NCl/SiO_2$, $PdCl_2$–$CoCl_2$–$(C_4H_9)_4NCl/SiO_2$, $PdCl_2$–$CuCl_2$–$(C_4H_9)_4NCl/SiO_2$, and two $PdCl_2$–$CoCl_2$–$CuCl_2$–$(C_4H_9)_4NCl/SiO_2$ catalysts with different $PdCl_2$ concentration, indicate in all cases high initial activities for the hydrodechlorination of CCl_4 in a H_2 atmosphere at 130°C. However, the $PdCl_2$–$(C_4H_9)_4NCl/SiO_2$ base catalyst with 2 wt% Pd tends to deactivate appreciably with time. Doping $CoCl_2$ into the $PdCl_2$–$(C_4H_9)_4NCl/SiO_2$ catalyst enhances its initial CCl_4 conversion and the specific reaction rate, shifts the reaction toward formation of more hydrocarbons, and also prolongs the life of the catalyst. Addition of $CuCl_2$ to the $PdCl_2$–$(C_4H_9)_4NCl/SiO_2$ catalyst also improves the initial CCl_4 conversion and the specific rates and has an even stronger stabilizing effect on the maintenance of the catalytic activity. When both $CoCl_2$ and $CuCl_2$ are added to the base catalyst, they show a synergistic effect as the promoted catalyst exhibits the highest CCl_4 initial conversion and the greatest longevity among all four catalysts. The product distribution is also shifted to some extent from hydrocarbons to partially hydrodechlorinated chlorocarbons. The second $PdCl_2$–$CoCl_2$–$CuCl_2$–$(C_4H_9)_4NCl/SiO_2$ catalyst with four times lower $PdCl_2$ concentration has lower specific activity but higher turnover frequency than the first catalyst, indicating more efficient use of $PdCl_2$. The observed promotional effects are attributed to interactions between Pd-containing active centers with either $CoCl_2$ or $CuCl_2$ or both, resulting in more stable active centers. These modified active centers are expected to have less tendency to cause oligomerization or polymerization of CCl_4 to form polychlorocarbons or coke which lead to catalyst deactivation.

ACKNOWLEDGMENTS

The authors acknowledge the financial support for this research by the Department of Energy through Contract TTP CH_2-2-11-04. The authors also thank Micromeritics for the partial support in the acquisition of equip-

ment used for physical characterization and the PQ Corporation for the donation of silica support, Dr. L. Teesch and Ms. D. Lamb for assistance in performing the GC-MS analysis, and Dr. Christopher J. Brooks for his valuable comments.

REFERENCES

1. Weiss, A. H., Gambhir, B. S., and Leon, R. B., *J. Catal.* **22**, 245 (1971).
2. Weiss, A. H., Valinski, S., and Antoshin, G. V., *J. Catal.* **74**, 136 (1982).
3. Roberts, D. J., and Kahokola, K. V., *Anal. Proc.* **23**, 437 (1986).
4. Getty, E. E., Petrosius, S. C., and Drago, R. S., *J. Mol. Catal.* **67**, 127 (1991).
5. Datta, R., and Rinker, R. G., *J. Catal.* **95**, 181 (1985).
6. Datta, R., Savage, W., and Rinker, R. G., *J. Catal.* **95**, 193 (1985).
7. Datta, R., Rydant, J., and Rinker, R. G., *J. Catal.* **95**, 202 (1985).
8. Rony, P. R., *Ann. NY Acad. Sci.* **172**, 238 (1970).
9. Kenny, C. N., *Catal. Rev. Sci. Eng.* **11**, 197 (1975).
10. Livbjerg, H., Jensen, K. F., and Villadsen, J., *J. Catal.* **45**, 216 (1976).
11. Buchanan, A. C., III, Dworkin, A. S., and Smith, G. P., *J. Am. Chem. Soc.* **105**, 2843 (1983).
12. Rao, V., and Datta, R., *J. Catal.* **114**, 337 (1988).
13. Janz, G. J., "Molten Salts Handbook." Academic Press, New York, 1967.
14. Bloom, H., "The Chemistry of Molten Salts." Benjamin, New York, 1967.
15. Parshall, G. W., *J. Am. Chem. Soc.* **94**, 8716 (1972).
16. Dafinger, W., and Schmidhammer, L., European patent 0,523,553 A1, (1991).
17. Anderson, J. R., and Pratt, K. C., "Introduction to Characterization and Testing of Catalysts," p. 355. Academic Press, San Diego, 1985.
18. (a) Noelke, C. J., and Rase, H. F., *Ind. Eng. Chem. Prod. Res. Dev.* **18**, 325 (1979); (b) Rossin, J. A., and Farris, M. M., *End. Eng. Chem. Res.* **32**, 1024 (1993).
19. Manson, W. R., III, and Grey, H. B., *J. Am. Chem. Soc.* **90**, 5721 (1968).
20. Assher, M., and Vofsi, D., *J. Chem. Soc. B* 947 (1968).
21. Anju, Y., Mochida, I., Yamamoto, H., Kato, A., and Seyama, T., *Bull. Chem. Soc. Jpn.* **25**, 2319 (1972).
22. Letuchii, Ya. A., Lavrentiev, I. P., and Khidekel, M. L., *Oxid. Commun.* **6**, 285 (1985).